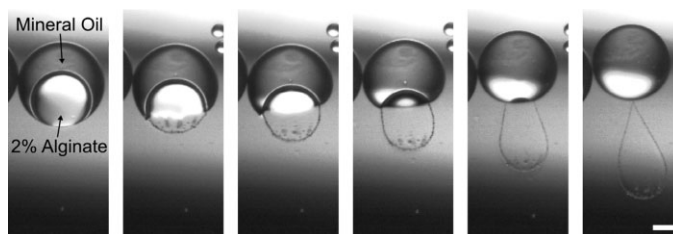


A Microfluidic Approach to Encapsulate Living Cells in Uniform Alginate Hydrogel Microparticles

Carlos J. Martinez,* Jin Woong Kim,* Congwang Ye, Idelise Ortiz, Amy C. Rowat, Manuel Marquez, David Weitz

A microfluidic technique is described to encapsulate living cells in alginate hydrogel microparticles generated from monodisperse double-emulsion templates. A microcapillary device is used to fabricate double emulsion templates composed of an alginate drop surrounded by a mineral oil shell. Hydrogel formation begins when the alginate drop separates from the mineral oil shell and comes into contact with Ca^{2+} ions in the continuous phase. Alginate hydrogel microparticles with diameters ranging from 60 to 230 μm are obtained. 65% of the cells encapsulated in the alginate microparticles were viable after one week. The technique provides a useful means to encapsulate the living cells in monodisperse hydrogel microparticles.



Prof. C. J. Martinez, C. Ye

School of Materials Engineering, Purdue University, 701 West Stadium Avenue, West Lafayette, IN 47907-2045, USA

E-mail: cjmartinez@purdue.edu

Prof. J. W. Kim

Department of Applied Chemistry, Hanyang University, 55 Hanyangdaehak-ro, Sangnok-gu, Ansan-si, Gyeonggi-do 426-791, Korea

E-mail: kjwoong@hanyang.ac.kr

I. Ortiz

Department of Cellular and Molecular Pharmacology, University of California San Francisco, San Francisco, CA 94158, USA

Prof. A. C. Rowat

Department of Integrative Biology and Physiology, University of California Los Angeles, Los Angeles, CA 90095, USA

Dr. M. Marquez

Department of Mechanical Engineering, 401 West Main Street, Room E3221, P.O. Box 843015, Richmond, VA 23284-3015, USA

Prof. D. Weitz

School of Engineering and Applied Sciences, Department of Physics, Harvard University, Cambridge, MA 02138, USA

1. Introduction

Hydrogel materials have been widely used as synthetic extracellular matrices for cell encapsulation and transplantation.^[1] Particularly, millimeter-sized hydrogel beads provide a three-dimensional hydrated structure that augments the mechanical integrity of the immobilized cells while simultaneously permitting the facile diffusion of nutrients and metabolites to and from the cells.^[2] The immobilized cells can act as micro-factories that produce hormones, such as insulin and growth factors.^[3] For this kind of applications, precise control over both hydrogel formation and cell density is needed. Also, the hydrogel materials should have affinity to the cells to provide sufficient cell viability. These requirements represent a challenge to both the medical and engineering communities.

Of all the synthetic and natural sources of hydrogel materials, alginate is attractive for encapsulating living cells. Alginate can be physically crosslinked to form a gel

phase with divalent ions.^[4] Alginate hydrogel beads have been easily fabricated by extruding drops of an alginate solution in air using a syringe and collecting these drops into a solution of divalent ions.^[3] Gelation begins immediately when the alginate drop comes into contact with the divalent ions in solution and continues until the whole bead is physically crosslinked as divalent ions diffuse from the continuous phase through the periphery of the drop. This simple technique has been used widely to encapsulate cells in alginate beads. However, it offers little control of drop formation, and leads to polydisperse millimeter-sized beads. Micrometer-sized beads provide higher mechanical strength, easier implantation, and better transport of oxygen and nutrients.^[5] This has spurred development of techniques that produce monodisperse hydrogel microparticles.

Drop generation techniques assisted by jetting air,^[6] electric field,^[7] and vibrating nozzle^[8] have decrease the alginate drop size and made its distribution relatively narrow. However, it is still difficult to generate microparticles with sufficient monodispersity to have a coefficient of variation less than 10%. Recently, some studies have exploited the drop generation capabilities of microfluidic devices. Using a T-junction device, monodisperse alginate drops are produced in micrometer length scales.^[9–12] The alginate drops are gelled by transferring into a divalent ion solution. Otherwise, gelation can be carried out via coalescence of alginate and aqueous Ca^{2+} drops in a microfluidic chamber.^[12–16] Internal gelation is another method that allows the gelation of alginate drops while they are dispersed in the oil phase.^[17–19] Although these methods produced smaller monodisperse alginate drops, precise control over the gelation process is complicated. Moreover, the removal of the immiscible fluid requires strong mechanical and chemical treatments, which prolongs exposure of the cells to divalent ions or solvents. Thus, effective encapsulation of cells in alginate hydrogel particles requires precise control of drop formation and gelation, and to safely harvest the gelled microparticles from the solvent mixture.

The aim of this study is to introduce a microcapillary device-based microfluidic technique to encapsulate living cells in monodisperse alginate hydrogel microparticles generated from double emulsion templates. Monodisperse double emulsion drops composed of an alginate droplet surrounded by a mineral oil drop dispersed in an aqueous CaCl_2 solution are generated in a microcapillary device.^[19] The oil drop serves as a carrier for the alginate drops as they are transported to and collected in a Ca^{2+} solution. Gelation occurs as the alginate drop separates from the mineral oil shell and contacts the Ca^{2+} ions in water. The feature of this approach is that unstable double emulsions are used as sacrificial payload carriers. This technique offers several advantages over other microfluidic techniques including

the self-separation of the alginate drop from the immiscible fluid as well as precise control of both drop formation and number of cells per hydrogel particle. The self-separation of the alginate drop enables harvesting of the alginate encapsulated cells without the need of a solvent and limits the amount of oil in the collection container.

2. Experimental Section

2.1. Fabrication of Microcapillary Devices

To fabricate microcapillary devices, first, a cylindrical glass capillary (outer diameter = 1.0 mm, World Precision Instruments, Sarasota, Florida) was fitted in a micropipette puller (Model P-97, Sutter Instruments, Novato, CA, USA). Heating and pulling under the tension breaks the glass capillary into two equal sized, tapered capillaries. The tapered glass capillaries were then cleaved to the desired final diameters using a forge station (Microforge, MF 830, Narishige, Japan). Typical diameters of the input (d_{input}) and exit (d_{exit}) capillaries ranged from 20 to 300 μm . The round capillaries were then inserted and aligned in a square capillary. Choosing the outer diameter of the round capillaries to be the same as the width of the square capillary facilitates alignment. Three 20G luer-stubs (Intramedic Luer Stub Adapters, Beckton Dickinson, Sparks, MD, USA) serve as input connectors for the fluids. A schematic of the microcapillary device and the region of the device where the two tapered capillaries meet are shown in Figure 1a and b, respectively.

2.2. Preparation of Fluids

Three solutions (inner, middle, and outer) were prepared to generate the double emulsions in the microcapillary devices. The inner fluid was prepared by dissolving alginic acid sodium salt from brown algae (100–300 cP, 2 wt% at 25 °C, M/G ratio ≈ 1.96) in deionized water. A mixture of 0.4 wt% Span 80 surfactant in light

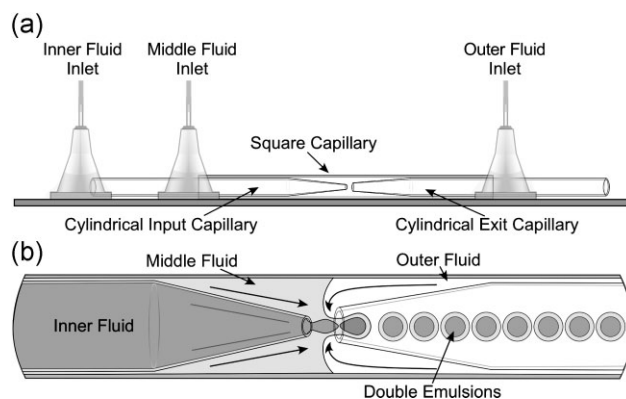


Figure 1. Schematic illustrations of (a) microcapillary device and (b) the region of the device where the input and exit capillaries meet. Note that the middle and outer fluids flow in opposite directions within the gap between the round and square capillaries while the inner fluid flows from the interior of the input capillary. Drops are formed and collected in the exit capillary.

mineral oil was used as the middle fluid. A mixture of 0.5 wt% Tween 20 surfactant, 40 wt% glycerol and 59.5 wt% deionized water served as the outer fluid. Double emulsions were collected in a 0.100 M aqueous solution of CaCl_2 with 2 wt% P123 Pluronic surfactant that was added to improve the stability of the mineral oil in the CaCl_2 solution. All chemicals were used as received and obtained from Sigma-Aldrich (Saint Louis, MA, USA), except the P123, which was obtained from Dow Chemicals (Atlanta, GA, USA).

2.3. Generation of Monodisperse Double Emulsions

To fabricate double emulsions the inner, middle, and outer fluids were loaded into glass syringes (Hamilton Gastight, Hamilton Co., Reno, NV, USA). The syringes were connected to the luer-stub inputs using polyethylene PE-5 tubing with an outer diameter of 1.32 mm and inner diameter of 0.86 mm (Scientific Commodities, Lake Havasa City, AZ, USA). Syringe pumps (PHD 2000, Harvard Apparatus, Holliston, MA, USA) were used to control the fluid flow rates. Droplet production was visualized in an inverted microscope (DM-IRBE, Leica, Germany) equipped with a fast-camera (Phantom V9, Vision Research, Wayne, NJ, USA) capable of up to 5.5×10^4 frames \cdot s $^{-1}$. Double emulsions were generated by individually adjusting the flow rates of the three fluids.

2.4. Encapsulation of Yeast Cells

Yeast cells (PDC1-GFP, *Saccharomyces cerevisiae*) were inoculated from a single colony and grown overnight in yeast extract peptone dextrose (YPD) at 30 °C. A 10 mL aliquot of the master stock culture was diluted in 5 mL of YPD and cultured for 24 h at 30 °C. Cell growth was plateaued at a density of $\text{OD}_{600} = 0.45$, which corresponds to $\approx 10^7$ cells \cdot mL $^{-1}$. The cells were then washed four times in YPD and re-suspended in a 2 wt% alginate/tris buffer solution. The viscous alginate/cell solution was tumbled in a rotary wheel (Glas-Col, Terre Haute, IN, USA) for 15 min, followed by a dispersion step using an ultrasonicator (Fisher Scientific, St. Louis, MO, USA) to break up cell aggregates. The cell/alginate solution was then loaded into a glass syringe for incorporation into the double emulsion. A live/dead assay (LIVE/DEAD Fixable Red Dead Cell Stain Kit, Invitrogen, Carlsbad, CA, USA) was used to check cell viability after encapsulation. Using molecular probes designed to ensure accurate assessment of cell viability enables to distinguish live cells from dead cells after the cells have been stained.

2.5. Observation of Hydrogel Microparticles

Carboxyl-terminated/rhodamine labeled *N*-isopropylacrylamide (NIPAM) microgels, with a hydrodynamic diameter of ≈ 200 nm, were added to the alginate solution at a concentration of 0.5 vol%, to image the hydrogels via confocal laser scanning microscope fitted with a 1 mW 543 nm laser (CLSM, Zeiss LSM510 META, Carl Zeiss North America, Thornwood, NY, USA). Since the fluorescent microgels have the same negative charge as the G-Block in the alginate, they are embedded in the alginate network during gelation. Then, the fluorescently labeled alginate hydrogel microparticles were imaged. To analyze the shape and volume of the microparticles, we reconstructed their three-dimensional images from CLSM z-stack images. A z-stack of images was obtained for 20

fluorescently labeled alginate hydrogel microparticles in water. Each image of the stack (with a 0.7 μm z-step) was subject to a mean filter that smoothed out the hydrogel area. Each slice was then thresholded and the hydrogel area for each slice was found. After compiling each slice, a projected fluorescence image of the alginate hydrogel particles was obtained.

3. Results and Discussion

3.1. Double Emulsion Templating to Fabricate Hydrogel Microparticles

Uniform alginate hydrogel microparticles were fabricated using the double emulsion template consisting of the aqueous alginate core and mineral oil shell. The double emulsion droplets were generated in the microcapillary device. The coaxial geometry of the device enables fabrication of double emulsions in a single step. The inner fluid flows through the inner capillary while the outer and middle fluids are pumped from the opposite direction along the gap between the round and square capillaries (Figure 1b). As the three fluids are forced through the exit capillary, the inner and middle fluids break into monodisperse double emulsion drops. Before gelation, the mineral oil shell protects the alginate solution; during gelation, however, the shell is open to transport the aqueous alginate drop into the CaCl_2 solution. The double emulsion drops generated at the entrance of the exit capillary are shown in Figure 2a. It can be observed that the inner and outer drops are uniform in size. A 2.5% CV was obtained via image analysis for both the inner and outer drops. Neither coalescence of oil drops, nor premature separation of the inner drop was observed while they traverse the exit capillary toward the CaCl_2 solution.

3.2. Effect of Microcapillary Device Geometry on Drop Formation

Both inner and outer drop diameters can be varied independently by changing flow rates and the round capillary diameter. To understand the effects of these variables, double emulsion drops were generated in microcapillary devices with different geometries and by independently varying the fluid flow rates. Then, through image analysis the inner and outer diameters were measured for each device and flow rate combinations. A plot of the ratio of the inner drop diameter (d_{inner}) and the exit capillary diameter (d_{exit}) as a function of the ratio between the outer flow rate (Q_{outer}) to the sum of the inner (Q_{inner}) and middle (Q_{middle}) flow rates is shown in Figure 2b. The inner drop diameter changes from 0.8 to 1.2 times d_{exit} for the different device geometries over a 2.5–17 flow rate ratio. This means d_{inner} does not change significantly with increasing Q_{outer} . This behavior is different from that

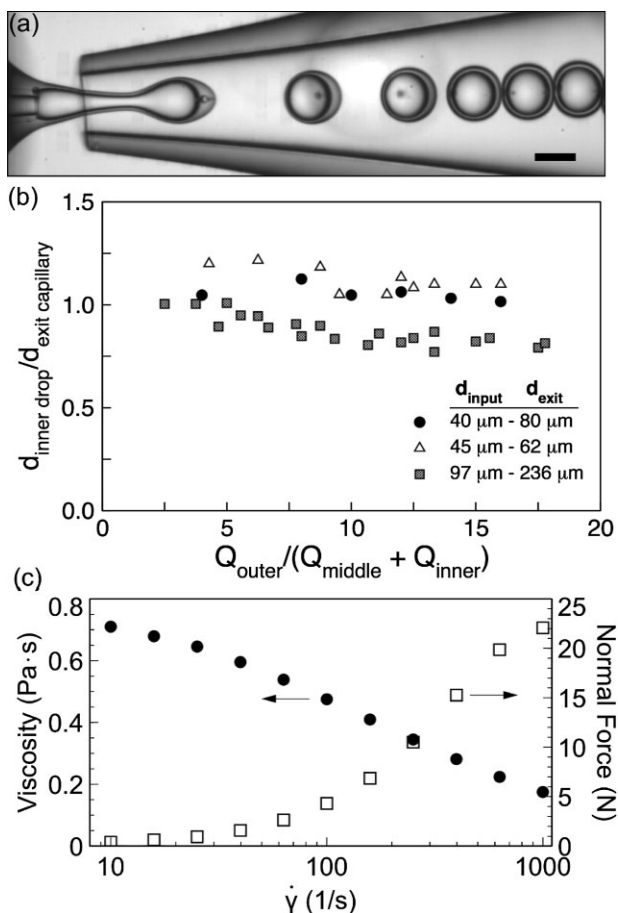


Figure 2. (a) Optical image of alginate/mineral oil double emulsion drop formation near the entrance of the exit capillary. The device dimensions are $d_{\text{input}} = 40 \mu\text{m}$ and $d_{\text{exit}} = 109 \mu\text{m}$. The flow rates of the inner, middle, and outer fluids are $Q_{\text{inner}} = 300 \mu\text{L} \cdot \text{h}^{-1}$, $Q_{\text{middle}} = 800 \mu\text{L} \cdot \text{h}^{-1}$, and $Q_{\text{outer}} = 10\,000 \mu\text{L} \cdot \text{h}^{-1}$. (b) The ratio of the inner drop diameter and the exit capillary diameter as a function of the ratio between Q_{outer} and the sum of Q_{middle} and Q_{inner} for different device geometries. (c) Viscosity and normal force as a function of shear rate ($\dot{\gamma}$) for a 2wt% alginate solution. The scale bar in (a) is $100 \mu\text{m}$.

observed by Utada et al.^[19] and Ye et al.^[20] for Newtonian fluids, where increasing Q_{outer} leads to a significant reduction in the inner and outer drop diameters. We can attribute this behavior to the rheological properties of the alginate solutions. Alginate solutions exhibit a viscoelastic shear thinning behavior as shown in Figure 2c. Apparent viscosity (η_{app}) at a shear rate ($\dot{\gamma}$) of 10 s^{-1} is $0.78 \text{ Pa} \cdot \text{s}$; however, it decreases to $0.18 \text{ Pa} \cdot \text{s}$ at a $\dot{\gamma}$ of 1000 s^{-1} . The mineral oil and the aqueous outer fluid are both Newtonian, with a η_{app} of 1.4×10^{-3} and $3.0 \times 10^{-3} \text{ Pa} \cdot \text{s}$, respectively. The alginate solution has a viscosity two orders of magnitude higher than the outer fluid, effectively reducing the flow focusing capabilities of the outer fluid. These results agree with previous work by Nie et al.^[21] which

showed that the diameter of drops with made high viscosity solutions have a weaker dependence with increasing Q_{outer} . Additionally, Figure 2c shows an increase in solution normal force with increasing $\dot{\gamma}$. The normal force stems from the alginate chains reconfiguration under the applied shear rate as it flows through a reduced area, hence higher shear, at the entrance of the exit capillary.^[22,23] A normal force of 22 N was measured at the $\dot{\gamma}$ of 1000 s^{-1} as shown in Figure 2c. The normal force will work against the outer fluid shear stress as the fluids merge at the entrance of the exit capillary. The insensitivity of the inner solution to Q_{outer} provides significant stability in the drop generation once the optimal flow rate ratios are established.

3.3. Separation of Alginate Drops from the Double Emulsion Template

Once the double emulsions are generated, they were collected in a 0.100 M CaCl_2 solution. Even though Span 80 offers a window of inner drop stability, the inner alginate drop begins to separate from the mineral oil shell in 4 min. A time series image of the inner drop separation from the outer mineral oil drop is shown in Figure 3. The image shows a side-view of a double emulsion drop. In the initial stage, the inner drop is off-center since it is denser than the surrounding oil shell. A thin layer of mineral oil separates the bottom of the alginate drop from the continuous phase. A hole opens within the thin oil layer and expands to a diameter equal to the inner drop diameter. The gelation process initiates as soon as the alginate comes in contact with the CaCl_2 solution. The separation continues as the line tension between the oil and the alginate exerts a force that “squeezes” the inner drop out. Since the interfacial tension between the two aqueous fluids is low, there is not a driving force to restore the drop spherical shape and the hydrogel acquires a tear-drop shape. The inner drop is fully separated after 100 ms and complete gelation occurs after 3 min.

3.4. Imaging and Characterization of Alginate Hydrogel Microparticles

The hydrogel particles maintained their tear-drop shape after the separation process since there is no appreciable interfacial tension between the particles and the continuous phase; otherwise, reshaping would occur into a spherical shape. Furthermore, the thin crosslinked alginate layer already formed at the periphery of the alginate drop is more resistant to deformation. Initially the separated drops are buoyant since they are less dense ($1.03 \text{ g} \cdot \text{mL}^{-1}$) than the continuous phase ($1.05 \text{ g} \cdot \text{mL}^{-1}$). However, once they are fully gelled, they sediment to the bottom of the collection vessel. This self-separation between the inner drop and mineral oil shell not only facilitates hydrogel formation but also enables the easy removal of the immiscible fluid and

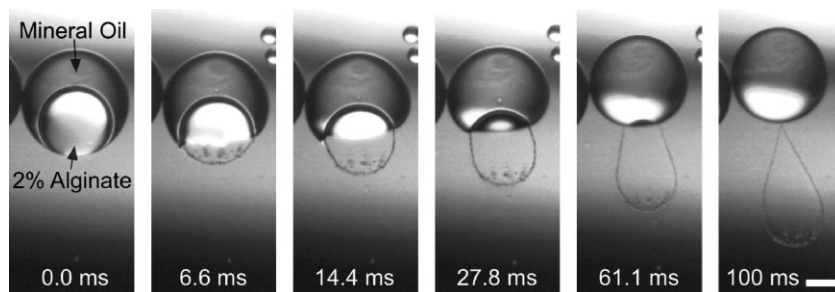


Figure 3. Time series of optical images showing the separation of the inner alginate drop from the mineral oil shell. The scale bar is 100 μm .

the replacement of the CaCl_2 solution with deionized water or a cell-friendly buffer solution. Bright field images of fully gelled alginate hydrogel microparticles in water are shown in Figure 4a and b. These images demonstrate that large and small hydrogel microparticles with uniform size can be fabricated using this technique. To confirm the monodispersity of these hydrogel microparticles, their three-dimensional shape was reconstructed from CLSM z-stack images. A projected fluorescence image of the alginate hydrogel particles is shown in Figure 4c. The total hydrogel volume was calculated by summing the volume each slice as follows:

$$V_{\text{hydrogel}} = \sum_{i=1} A_i Z_{\text{step}}$$

where V_{hydrogel} is the hydrogel volume, A_i the hydrogel area in each slice, and Z_{step} is the thickness of the slice. A plot

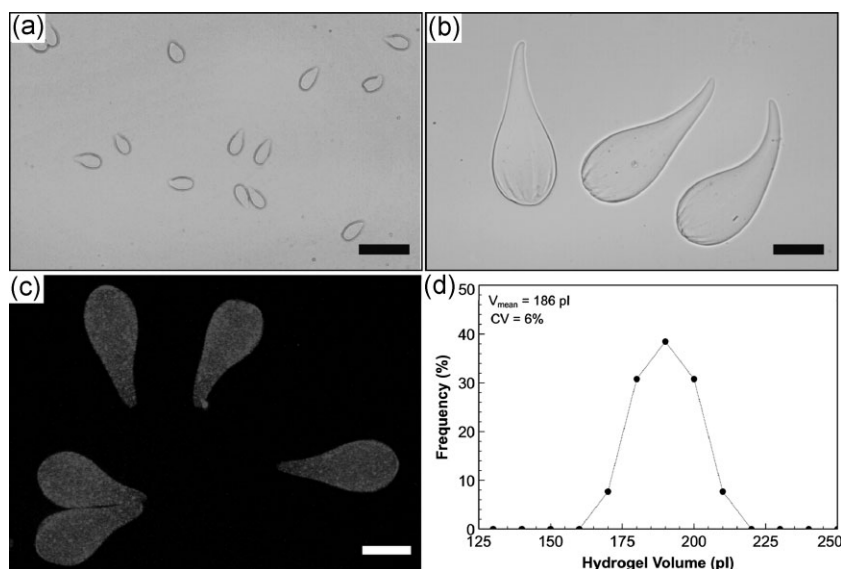


Figure 4. Bright field images of alginate hydrogel microparticles obtained from the double emulsion template with an inner drop diameter of (a) 62 and (b) 226 μm . (c) Confocal laser scanning microscope image of alginate hydrogel microparticles. (d) Volume distribution of hydrogel microparticles obtained via confocal volume reconstructions. Scale bars in (a) and (b) are 400, and (c) 50 μm , respectively.

of the distribution of hydrogel volumes, obtained from the reconstructed three-dimensional images, is shown in Figure 4d. The mean hydrogel volume is 186 pL with a CV of 6%, confirming that the hydrogel particles are uniform size. In certain situations a spherical hydrogel shape is preferred over the tear-drop shape. It is expected that a simple modification of the procedure will permit the generation of spherical alginate microparticles; e.g., partial gelation of the inner drop surface, caused by diffusion of undissociated divalent salt from the oil shell^[18] can give sufficient mechanical strength for curvature deformation of the escaping drop. This will help the drop to maintain its spherical shape while it separates from the outer oil shell. These modifications to the technique will be tested in future work.

3.5. Encapsulation and Viability of Yeast Cells in Hydrogel Microparticles

By using yeast cells as a simple model system, we tried to demonstrate the ability of the technique to encapsulate living cells. Yeast cells were added to the alginate solution and drops with $d_{\text{inner}} \approx 60 \mu\text{m}$ and $d_{\text{outer}} \approx 72 \mu\text{m}$ were produced at a rate of 250 Hz. While fabricating the alginate hydrogel microparticles, it was found that the medium property of collection solution affected the stability of hydrogel phase. Synthetic dextrose and YPD media are commonly used for culturing yeast instead of tris buffer.^[24] However, those two media swelled and eventually dissolved the alginate hydrogel in a week. We did not encounter this problem, when 1 \times tris buffer was used. A bright field optical image of a group of yeast cells encapsulated in alginate hydrogel microparticles is shown in Figure 5a. The cells appear as bright spots within the tear-drop shape delineating the hydrogel volume. The viability of yeast cells in the microparticles was observed using the live/dead assay. Over 98% of the cells were alive after the encapsulation and washing process and over 65% were alive after one week of encapsulation and incubation in 1 \times tris buffer media. The cell distribution in the hydrogels was quantified by performing a series of encapsulation experiments, with alginate solutions having different cell densities, 5×10^6 ,

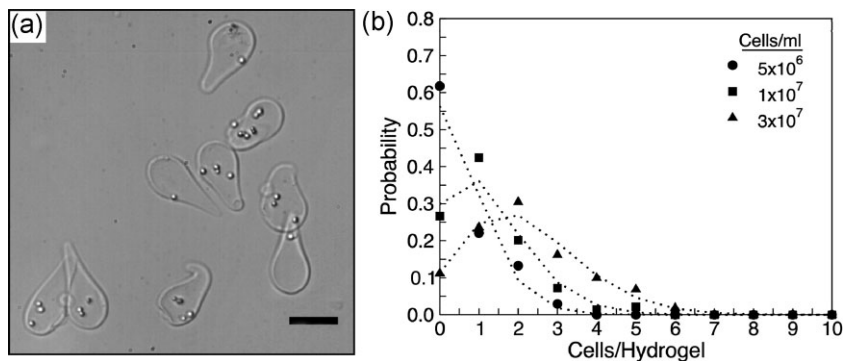


Figure 5. (a) Optical image of yeast cells encapsulated in hydrogel microparticles. The yeast cells appear as bright spots within the tear-drop shaped hydrogel microparticles. The scale bar is 50 μm . (b) Number distribution of the yeast cells per hydrogel particle. Dotted lines are the corresponding Poisson distribution for each cell density.

by the Purdue Research Fund. This work was also supported by the research fund of Hanyang University (HY-2011-N).

Received: September 6, 2011; Revised: November 18, 2011; Published online: February 7, 2012; DOI: 10.1002/mabi.201100351

Keywords: alginate hydrogels; cells; double emulsions; encapsulation; microfluidics

1×10^7 , 3×10^7 cells \cdot mL⁻¹. The inner drop diameter was kept constant at 60 μm for all encapsulation experiments. The distribution of yeast cells in the hydrogel particle with different cell densities is shown in Figure 5b. The number of cells per hydrogel particle for the three concentrations followed a Poisson distribution.

4. Conclusion

In summary, we have developed a technique to generate monodisperse alginate hydrogel microparticles from the alginate/mineral oil double emulsion. This technique relies on tailoring the stability of the double emulsion droplets to control the self-separation of the inner alginate drop from the mineral oil shell. This study demonstrated that this approach is advantageous for cell encapsulation, since it not only enables the fabrication of uniform hydrogel microparticles in smaller length scales, but also allows control over the population of living cells in the microcapsules. The technique is not limited to alginate solutions and can be easily modified to fabricate hydrogel particles using other crosslinking chemistries. For example, we have been able to generate monodisperse poly(ethylene glycol) acrylate particles via UV photo-crosslinking (data not shown). The gentle nature of the inner drop separation permits the fabrication of soft hydrogel particles that otherwise will be degraded during the cleaning process. This technique can be valuable for encapsulation experiments that require a high level of biocompatibility and great control of hydrogel volume and cell concentration. Potential research applications include tissue engineering, harvesting and identification of cell factors, and single-cell studies.

Acknowledgements: C. M. was supported by an International Network of Emerging Science and Technology. C. Y. was supported

- [1] R. P. Lanza, J. L. Hayes, W. L. Chick, *Nat. Biotechnol.* **1996**, *14*, 1107.
- [2] J. A. Rowley, G. Madlambayan, D. J. Mooney, *Biomaterials* **1999**, *20*, 45.
- [3] R. V. Schilfgarde, P. Vos, *J. Mol. Med.* **1999**, *77*, 199.
- [4] K. Y. Lee, D. J. Mooney, *Chem. Rev.* **2001**, *101*, 1869.
- [5] D. Chicheportiche, G. Reach, *Diabetologia* **1988**, *31*, 54.
- [6] U. Prube, B. Fox, M. Kirchhoff, F. Bruske, J. Breford, K. D. Vorlop, *Biotechnol. Tech.* **1998**, *12*, 105.
- [7] B. Bugarski, Q. Li, M. F. A. Goosen, D. Poncelet, R. J. Neufeld, G. Vunjak, *AIChE J.* **1994**, *40*, 1026.
- [8] S. B. Huang, M. H. Wu, G. B. Lee, *Sens. Actuators. B: Chem.* **2010**, *147*, 755.
- [9] L. Capretto, S. Mazzitelli, C. Balestra, A. Tosi, C. Nastruzzi, *Lab Chip* **2008**, *8*, 617.
- [10] K. S. Huang, T. H. Lai, Y. C. Lin, *Front. Biosci.* **2006**, *12*, 3061.
- [11] D. Ogończyk, M. Siek, P. Garstecki, *Biomicrofluidics* **2011**, *5*, 013405.
- [12] C. H. Yeh, Q. Zhao, S. J. Lee, Y. C. Lin, *Sens. Actuators, A: Phys.* **2009**, *151*, 231.
- [13] T. Braschler, R. Johann, M. Heule, L. Metref, P. Renaud, *Lab Chip* **2005**, *5*, 553.
- [14] K. Liu, H. J. Ding, J. Liu, Y. Chen, X. Z. Zhao, *Langmuir* **2006**, *22*, 9453.
- [15] V. Trivedi, E. S. Ereifej, A. Doshi, P. Sehgal, P. J. Vandevord, A. S. Basu, *Engineering in Medicine and Biology Society, 2009. EMBC 2009. Annual International Conference of the IEEE* **2009**, p. 7037.
- [16] S. Sugiura, T. Oda, Y. Izumida, Y. Aoyagi, M. Satake, A. Ochai, N. Ohkohchi, M. Nakajima, *Biomaterials* **2005**, *26*, 3327.
- [17] W. H. Tan, S. Takeuchi, *Adv. Mater.* **2007**, *19*, 2696.
- [18] H. Zhang, E. Tumarkin, R. Peerani, Z. Nie, R. M. Sullan, G. C. Walker, E. Kumacheva, *J. Am. Chem. Soc.* **2006**, *128*, 12205.
- [19] A. S. Utada, E. Lorenceau, D. R. Link, P. D. Kaplan, H. A. Stone, D. Weitz, *Science* **2005**, *308*, 537.
- [20] C. Ye, A. Chen, P. Colombo, C. Martinez, *J. R. Soc. Interface* **2010**, *7*, S461.
- [21] Z. Nie, M. Seo, S. Xu, P. C. Lewis, M. Mok, E. Kumacheva, G. M. Whitesides, P. Garstecki, H. A. Stone, *Microfluid. Nanofluid.* **2008**, *5*, 585.
- [22] A. J. M. Segeren, J. V. Boskamp, M. v. d. Tempel, *Faraday Discuss. Chem. Soc.* **1974**, *57*, 255.
- [23] M. H. Wagner, *Rheol. Acta* **1976**, *15*, 136.
- [24] F. Sherman, *Methods Enzymol.* **1991**, *194*, 21.